Role of Strontium in Oxide Epitaxy on Silicon (001)

J. W. Reiner,[1,*] K. F. Garrity,[2] F. J. Walker,[1] S. Ismail-Beigi,[1,2] and C. H. Ahn[1,2]

[1]*Department of Applied Physics, Yale University, New Haven, Connecticut 06520-8284, USA*
[2]*Department of Physics, Yale University, New Haven, Connecticut 06520-8120, USA*

(Received 4 May 2008; published 4 September 2008)

Epitaxial oxide-Si heterostructures, which integrate the functionality of crystalline oxides with Si technology, are made possible by a submonolayer of Sr deposited on Si (001). We find by electron diffraction studies using single termination Si wafers that this Sr submonolayer replaces the top layer of Si when deposited at 650 °C. Supported by first-principles calculations, we propose a model for the reaction dynamics of Sr on the Si surface and its effect on oxide epitaxy. This model predicts, and we experimentally confirm, an unexplored 25 °C pathway to crystalline oxide epitaxy on Si.

DOI: 10.1103/PhysRevLett.101.105503 PACS numbers: 68.47.Fg, 61.05.jh, 71.15.Mb, 81.15.Hi

Epitaxial oxides on Si have attracted considerable attention over the past decade, in part because of the need to replace SiO_2 as the dielectric layer in field effect transistors in order to continue Moore's law scaling. Crystalline oxide-Si heterostructures also integrate the rich functionality present in crystalline oxides, such as magnetism, ferroelectricity, and superconductivity, with modern Si device technology. To fully realize the potential of this functionality, the interface must be atomically abrupt between the two layers despite differences in bonding, chemistry, and coordination. The first heterostructures of this type were based on creating a submonolayer of Sr on the Si (001) surface at high temperature [1]. While this growth procedure has been expanded to allow the use of other elements, such as Ba or Ca [2], the combination of alkaline earth submonolayer deposition and Si temperature near 650 °C is, to date, the only pathway to epitaxial oxide growth directly on Si (001).

The role of Sr in enabling oxide heteroepitaxy has attracted broad theoretical and experimental interest. Theoretical studies predict that the optimal coverage of Sr on the Si surface for epitaxial oxide growth is $\frac{1}{2}$ monolayer (ML), forming a 2×1 surface structure [3]. The stability of $SrTiO_3$ films grown on such a structure has been calculated from first principles [4,5]. Experiments indicate that Sr coverages between $\frac{1}{4}$ and $\frac{1}{2}$ ML are suitable for epitaxial oxide growth [6]. However, the correspondence between experimental results and theoretical predictions regarding submonolayer Sr surface ordering is incomplete. In addition, the role of temperature in creating a suitable Sr template for oxide epitaxy is unexplained.

We have addressed these questions through a combination of experimental and theoretical studies and discovered a reaction of Sr with the Si surface that explains the structure formed by Sr on the Si surface, its dependence on temperature, and its role in oxide epitaxy on Si. The experiments consist of the deposition of Sr on 4° miscut Si wafers studied by *in situ* reflection high energy electron diffraction (RHEED). While regular Si wafers have a mixed surface termination, these miscut Si wafers have only a single surface termination due to the energy cost of dimer row-step ledge alignment [7], removing a key source of ambiguity in RHEED interpretation. We find that, when deposited on a high temperature Si surface, $\frac{1}{2}$ ML of Sr replaces the top layer of Si atoms, which migrate to step ledges. This high temperature Sr phase has been the basis for oxide epitaxy on Si to date. A symmetrically equivalent surface structure is formed on a static Si surface when $\frac{1}{2}$ ML Sr is deposited at room temperature. This surface structure also supports oxide epitaxy and represents an unexplored pathway to crystalline oxides on Si. First-principles density functional theory (DFT) calculations identify a key stable Sr surface structure at $\frac{1}{6}$ ML coverage, where each Sr atom replaces two Si dimers. This $\frac{1}{6}$ ML Sr structure, while incompatible with epitaxial oxide growth, is central to understanding how temperature affects the role of Sr in oxide epitaxy.

The experiments were carried out in a custom oxide molecular beam epitaxy chamber with *in situ* RHEED. Typical background pressures during the experiments were 10^{-10} Torr. 2-inch-diameter Si (001) wafers with a 4° miscut along the [110] direction were loaded into the growth chamber and heated to 850 °C until a 2×1 RHEED pattern was seen, indicating the removal of the amorphous SiO_2 layer and formation of dimer rows. Temperatures were measured by a thermocouple after calibration by a pyrometer. On miscut wafers, RHEED confirmed that dimer rows ran orthogonal to step ledges. The wafers were then cooled to the deposition temperature desired. Sr was evaporated from an effusion cell. Flux calibration was accomplished with a quartz crystal monitor that could be moved into the substrate position. Typical Sr deposition rates were 1 ML/min. During deposition, RHEED patterns were recorded at an energy of 15 keV.

Previous RHEED studies of Sr deposition on Si (001) used regular Si wafers that exhibit equal fractions of two surface symmetries (2×1 and 1×2) related to the two surface terminations of the Si lattice, which differ by an odd number of Si monolayers. These studies have consistently found a $3\times$ structure at $\frac{1}{6}$ ML of Sr, which disappears near

$\frac{1}{4}$ ML coverage, replaced by a 2× structure [1,6]. In Fig. 1 (a), we present RHEED data collected on a regular Si wafer at 650 °C during Sr deposition showing this evolution of surface structure. While the details of this intensity curve depend on the diffraction conditions, we consistently observe many of the features present in Fig. 1(a). In particular, a sharp minimum is often seen near 0.2 ML for the 2× diffraction spots, while the 3× structure is extinguished near $\frac{1}{4}$ ML Sr coverage. These features have been used extensively in procedures to grow epitaxial oxide heterostructures [1], but there has not been a convincing explanation of their origin. The most common implicit assumption about the symmetry of the Sr-Si surface has been that it preserves the local symmetry of the original Si surface [3]; Sr deposited on Si (001)-2 × 1 forms a structure with the same 2 × 1 symmetry (i.e., no change of orientation). However, RHEED studies on mixed termination Si wafers cannot rule out that the unit cell orientation changes from 2 × 1 to 1 × 2 during Sr deposition.

Our RHEED studies of Sr deposition on 4° miscut Si (001) resolve these issues of surface symmetry determination. For miscut Si wafers, only a single termination and symmetry are present, removing the above ambiguity. Typical RHEED patterns for the miscut Si (001) surface at 650 °C with no Sr and after deposition of $\frac{1}{6}$ and $\frac{1}{3}$ ML of Sr are shown in Fig. 2 with important reciprocal space points circled. With single termination Si wafers, we can uniquely identify the $\frac{1}{6}$ and $\frac{1}{3}$ ML coverages as 2 × 3 and 1 × 2, respectively. RHEED intensities as a function of Sr coverage at 2 × 1, 2 × 3, and 1 × 2 points in reciprocal space are presented in Fig. 1(b), showing a 2 × 1 → 2 × 3 → 1 × 2 transition. The reaction of Sr with the Si surface at 25 °C is completely different than at 650 °C. As shown in Fig. 1(c), the only symmetry present during Sr deposition at 25 °C is 2 × 1, with no evidence of either 2 × 3 or 1 × 2 structures at any Sr coverage. At intermediate Si temperatures, we see a crossover between these low and high temperature behaviors, with the 2 × 3 and 1 × 2 symmetries beginning to emerge at 300 °C.

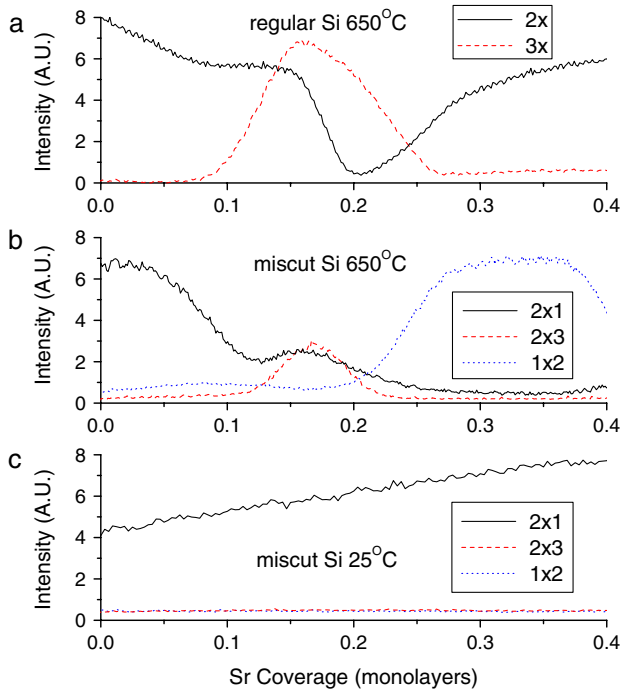

FIG. 1 (color online). RHEED intensity during Sr deposition of reciprocal lattice points related to 2 × 1, 2 × 3, and 1 × 2 symmetries on (a) regular Si (001) at 650 °C and miscut Si (001) at (b) 650 °C and (c) 25 °C.

We find that the minimum in 2× RHEED intensity observed at 650 °C on regular Si corresponds to the critical Sr coverage where the 1 × 2 symmetry emerges during deposition on miscut Si. The 2× spot intensity collected on a regular Si wafer, which has contributions from both Si surface terminations, should be similar to the sum of the 2 × 1 and 1 × 2 intensity curves for the miscut Si, as confirmed by the data in Fig. 1.

To determine the surface structures implied by these RHEED results, we perform first-principles DFT calculations using a plane-wave basis and norm-conserving pseudopotentials [8]. We use a slab geometry with at least eight layers of Si and symmetric Sr patterns on the two exposed surfaces. The nudged elastic band method with climbing images is employed to find energy barriers [9]. If we assume a static Si (001)-2 × 1 surface during Sr deposition, the most stable structure at $\frac{1}{6}$ ML consists of chains of Sr atoms, with the Sr filling trough sites between Si dimer rows, in agreement with earlier work [3]. While these chains can form a 2 × 3 structure at zero temperature, we expect a disordered surface without this symmetry at the experimental temperatures, since the energy cost for kinks in the chain to form is much less than kT. At $\frac{1}{2}$ ML Sr coverage, the most stable structure fills all trough sites and retains the 2 × 1 symmetry and orientation of the underlying Si surface, also in agreement with earlier work [3]. Since the miscut Si surface has 2 × 1 symmetry, this theoretical result explains the RHEED data at 25 °C, where we see a persistent 2 × 1 symmetry during $\frac{1}{2}$ ML Sr deposition [Fig. 1(c)].

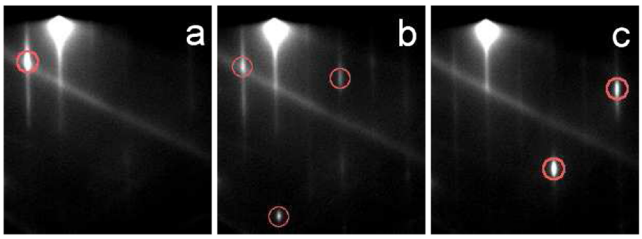

FIG. 2 (color online). RHEED images of miscut Si with surface coverages of (a) 0, (b) $\frac{1}{6}$, and (c) $\frac{1}{3}$ ML of Sr near the [110] azimuth showing a 2 × 1 → 2 × 3 → 1 × 2 transition. Reciprocal lattice points associated with 2 × 1 [(3/2, 0)], 2 × 3 [(3/2, 0), (1, 1/3), (0, 1/3)], and 1 × 2 [(0, 1/2), (−1, 1/2)] symmetries are circled in (a), (b), and (c), respectively. RHEED images near the [100] and [1$\bar{1}$0] azimuths show the same transition.

These results from DFT can also describe the 1×2 structure observed at 650 °C, but only if there is a transition of the symmetry of the Si surface from 2×1 to 1×2 during Sr deposition. A $2 \times 1 \rightarrow 1 \times 2$ transition of the Si surface occurs when the top layer of Si is removed, since this rotates the dimer bonds by 90°. Our RHEED results indicate that this movement of the top layer of Si is occurring during Sr deposition, but only at high temperature. While this requires a large rearrangement of the Si surface, a similar temperature-dependent rearrangement of the top layer of Si has been reported to occur during As deposition [10]. Removal of the top layer of Si has also been proposed to explain scanning tunneling microscopy studies of submonolayer Ba structures on Si (001) [11]. We also note that 650 °C is above the temperature necessary for step-flow homoepitaxy on Si (001) [12].

The DFT results above, while identifying stable 2×1 and 1×2 structures at $\frac{1}{2}$ ML Sr, cannot explain why the top layer of Si moves to form the 1×2 structure at high temperature or why 2×3 symmetry is observed at $\frac{1}{6}$ ML Sr. By allowing some Si to be missing from the surface layer in our first-principles DFT calculations, we find a new class of stable structures at $\frac{1}{6}$ ML Sr, lower in energy than the Sr chains above, that resolve both of these questions. These structures are formed by removing $\frac{2}{3}$ of the Si dimers, reconstructing the exposed subsurface Si atoms, and placing Sr into the vacancy sites, as shown in Fig. 3. The vacancy sites are similar to the DV-2 dimer vacancies observed on clean Si surfaces, which are stabilized by strain relief at finite temperature [13]. The 2×3 and $c(2 \times 6)$ structures at $\frac{1}{6}$ ML Sr are more stable by 0.14 eV/Sr and 0.19 eV/Sr, respectively, than those based on a static Si surface. The Sr atoms are arranged in lines flanked on both sides by dangling Si bonds, resulting in strong overlap of the Si and Sr orbitals. Based on analysis of the electronic states, we attribute the stability of the 2×3 and 1×2 structures to Sr-Si covalent bond formation and not simply electron donation from Sr to Si [3]. For these calculations, we use bulk Si as the reservoir, which is equivalent to the surface Si moving to step edges.

When going beyond $\frac{1}{6}$ ML Sr at 650 °C, the remaining Si surface dimers in the 2×3 structure are removed, leading to the stable 1×2 structure at $\frac{1}{2}$ ML Sr depicted in Figs. 3(c) and 3(e), consistent with the symmetry observed in Fig. 1(b). This 1×2 structure differs from the 2×1 structure formed at the same coverage and 25 °C only by the removal of a single layer of Si atoms, with the displaced Si migrating to step ledges. During this migration of Si atoms, single-layer atomic steps may form on the miscut Si wafer surface, leading to a gradual loss of the single termination surface. Such a process would explain the drop in intensity for the 1×2 structure above 0.4 ML Sr coverage seen in Fig. 1(b).

Our model of the 2×1, 2×3, and 1×2 surfaces requires mass transport of Si to occur at 650 °C, but not 25 °C. Since the 2×3 structure at $\frac{1}{6}$ ML Sr is responsible for this Si redistribution, we have determined the kinetic barriers to its formation in order to estimate reaction rates and understand this temperature dependence. We find that the presence of Sr reduces the energy barrier for Si dimer bond breaking from 1.29 eV for bare Si to 0.92 eV with $\frac{1}{4}$ ML Sr and 0.63 eV with $\frac{1}{2}$ ML Sr. This large barrier reduction stems from Sr passivating the Si dangling bonds in the transition state. Estimates from transition state theory using these barriers show that the Si dimer structure is frozen at room temperature for typical deposition times but highly mobile at 650 °C [14]. This result explains why the 2×3 structure at $\frac{1}{6}$ ML and the 1×2 structure at $\frac{1}{2}$ ML are observed only during high temperature Sr deposition, since they both require surface Si motion, while at room temperature only the 2×1 symmetry associated with the static Si surface is observed.

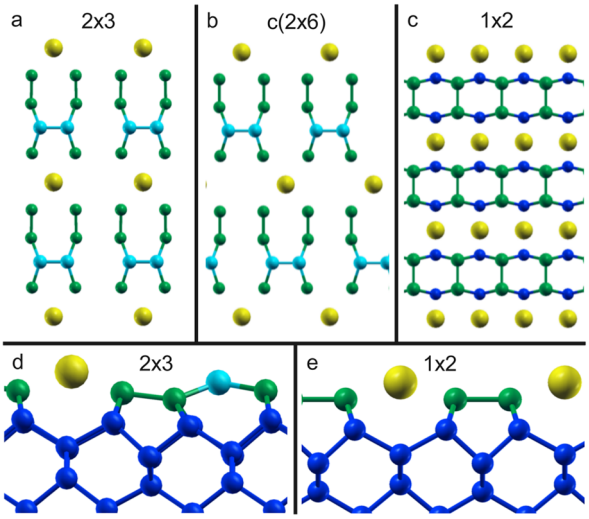

FIG. 3 (color online). Schematic top views of (a) 2×3 and (b) $c(2 \times 6)$ structures at $\frac{1}{6}$ ML Sr and (c) 1×2 structure at $\frac{1}{2}$ ML Sr and side views of (d) 2×3 and (e) 1×2 structures. The 2×3 structure has removed $\frac{2}{3}$ of the Si in the top layer. The 1×2 structure removes the remaining Si from the top layer. Sr—yellow, top Si—light blue, second Si—green, other Si—dark blue.

If $\frac{1}{2}$ ML of Sr forms the same structure at 650 °C and 25 °C, different only in that Sr replaces the top layer of Si in one case but not the other, oxide epitaxy should be possible on both structures. To date, there have been no reports of epitaxial oxide deposition on Si using a submonolayer Sr template deposited at room temperature. On regular Si wafers, we deposited $\frac{1}{2}$ ML Sr at 25 °C, 250 °C, and 650 °C and $\frac{1}{6}$ ML Sr at 650 °C. We then deposited 5 ML BaO films on each of these structures using the same growth procedure, with a Si temperature of 75 °C. RHEED images of the BaO surfaces were collected and are presented in Fig. 4. We see that for the three $\frac{1}{2}$ ML Sr samples excellent epitaxy is achieved for the 25 °C and 650 °C samples, while the 250 °C sample shows poor epitaxy with a much lower peak to background ratio. BaO growth on the $\frac{1}{6}$ ML Sr sample is amorphous [15]. We

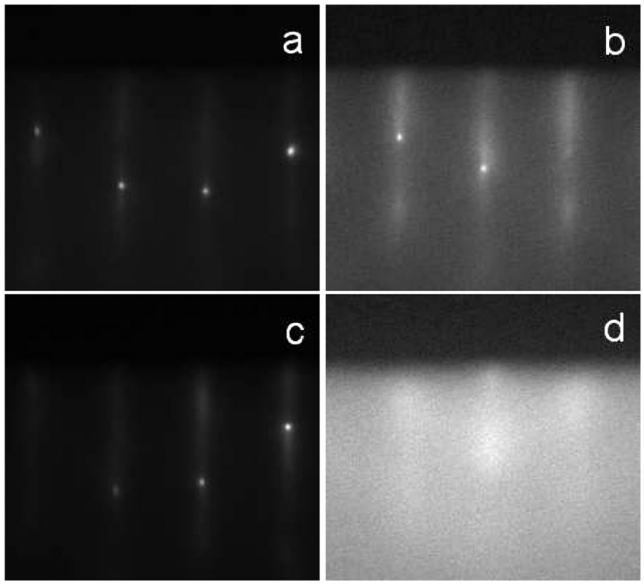

FIG. 4. RHEED images of 5 ML BaO films on Si (001) after $\frac{1}{2}$ ML deposition of Sr at (a) 25 °C, (b) 250 °C, and (c) 650 °C and (d) after $\frac{1}{6}$ ML deposition of Sr at 650 °C.

observe RHEED oscillations for all three $\frac{1}{2}$ ML Sr samples, but with significantly more damping for the 250 °C sample.

These results support our model of the surface reaction dynamics. At high temperatures, the 2×3 structure forms quickly at $\frac{1}{6}$ ML, leading to the complete replacement of the top layer of Si to form the 1×2 structure as the Sr coverage reaches $\frac{1}{2}$ ML. At room temperature, formation of the 2×3 structure is frozen out, so Sr atoms bond to the existing 2×1 Si dimer surface. Both of these processes create well-ordered surfaces that result in oxide epitaxy. At intermediate temperatures, the formation of the 2×3 structure and replacement of Si by Sr is only partial, leading to a surface more disordered than the previous two and not suited to oxide epitaxy. When only $\frac{1}{6}$ ML Sr is deposited at 650 °C, the resulting 2×3 structure is frozen into place at the BaO growth temperature of 75 °C, creating a substantially different surface structure that leads to amorphous growth. This model of Sr reaction dynamics on Si (001) explains the RHEED data on both miscut and regular Si wafers, the dramatic difference in the suitability for oxide epitaxy of the $\frac{1}{6}$ and $\frac{1}{4}$ ML Sr coverages when deposited at high temperature, and the role of Si temperature in enabling oxide epitaxy through both high and room temperature processes.

In conclusion, we have demonstrated through RHEED studies of Sr deposition on single termination miscut Si (001) surfaces and first-principles calculations that $\frac{1}{2}$ ML Sr deposited at high temperature (650 °C) replaces the top monolayer of Si, causing a $2 \times 1 \rightarrow 2 \times 3 \rightarrow 1 \times 2$ transition of the surface symmetry. This movement of Si is driven by the formation of a 2×3 structure at $\frac{1}{6}$ ML Sr, which removes $\frac{2}{3}$ of the surface Si atoms. Only when the Sr deposition is performed at room temperature do we see a persistent 2×1 symmetry consistent with a model where there is no movement of the top layer of Si. This room temperature Sr structure is symmetrically equivalent to the high temperature Sr structure and represents an unexplored pathway to crystalline oxide on Si heterostructures. Understanding the nature of these reactions with the Si surface has important implications for epitaxial oxide growth on Si, in both optimizing interface quality and expanding these growth techniques to other materials systems.

We acknowledge support from the National Science Foundation under MRSEC DMR 0520495 and DMR 0705799, along with support from SRC.

*james.reiner@yale.edu

[1] R. A. McKee, F. J. Walker, and M. F. Chisholm, Phys. Rev. Lett. **81**, 3014 (1998).
[2] R. A. McKee, F. J. Walker, M. B. Nardelli, W. A. Shelton, and G. M. Stocks, Science **300**, 1726 (2003).
[3] C. R. Ashman, C. J. Först, K. Schwarz, and P. E. Blöchl, Phys. Rev. B **69**, 075309 (2004).
[4] C. J. Först, C. R. Ashman, K. Schwarz, and P. E. Blöchl, Nature (London) **427**, 53 (2004).
[5] X. Zhang, A. A. Demkov, H. Li, X. Hu, Y. Wei, and J. Kulik, Phys. Rev. B **68**, 125323 (2003).
[6] J. Lettieri, J. H. Haeni, and D. G. Schlom, J. Vac. Sci. Technol. A **20**, 1332 (2002).
[7] O. L. Alerhand, A. N. Berker, J. D. Joannopoulos, D. Vanderbilt, R. J. Hamers, and J. E. Demuth, Phys. Rev. Lett. **64**, 2406 (1990).
[8] M. C. Payne, M. P. Teter, D. C. Allen, T. A. Arias, and J. D. Joannopoulos, Rev. Mod. Phys. **64**, 1045 (1992).
[9] G. Henkelman, B. P. Uberuaga, and H. Jonsson, J. Phys. Chem. **113**, 9901 (2000).
[10] O. L. Alerhand, J. Wang, J. D. Joannopoulos, E. Kaxiras, and R. S. Becker, Phys. Rev. B **44**, 6534 (1991).
[11] X. Hu, X. Yao, C. A. Peterson, D. Sarid, Z. Yu, J. Wang, D. S. Marshall, R. Droopad, J. A. Hallmark, and W. J. Ooms, Surf. Sci. **445**, 256 (2000); K. Ojima, M. Yoshimura, and K. Ueda, Surf. Sci. **491**, 169 (2001).
[12] A. J. Hoeven, E. J. Van Loenen, D. Dijkkamp, J. M. Lenssinck, and J. Dieleman, Thin Solid Films **183**, 263 (1989).
[13] J. Wang, T. A. Arias, and J. D. Joannopoulos, Phys. Rev. B **47**, 10 497 (1993).
[14] A. P. Smith and H. Jonsson, Phys. Rev. Lett. **77**, 1326 (1996).
[15] A.-B. Posadas, M. Lippma, F. Walker, M. Dawber, C. Ahn, and J.-M. Triscone, in *Physics of Ferroelectrics—A Modern Perspective* (Springer, New York, 2007), p. 284.